RSC Advances

PAPER

View Article Online
View Journal | View Issue

Cite this: *RSC Adv.*, 2026, **16**, 16887

Micro-array based on parafilm towards the opto-analysis of Cu(II), Cr(VI), and Ni(II) ions in fish samples by specific indicators: a state-of-the-art approach

Farnaz Bahavarnia,[ab] Houman Kholafazad Kordasht,[c] Mohammad Hasanzadeh *[b] and Nasrin Shadjou[d]

In this study, a parafilm-based colorimetric micro-array (PCMA) is introduced as a novel, low-cost sensor for the specific detection of copper (Cu(II)), chromium (Cr(VI)), and nickel (Ni(II)) ions in real samples. We developed a convenient and straightforward micro-array based on parafilm for creating hydrophobic and semi-hydrophobic areas for the colorimetric detection of three metal ions, namely, Cu(II), Cr(VI), and Ni(II) ions, using color picker software installed on a smartphone. The principle of detection in this innovative sensing platform was based on the chemical interactions of these metal ions with specific reagents. These interactions produced striking observable color changes that allowed for the easy identification and quantification of these targets in complex matrices. Based on the smartphone-supported digital image analysis, the prepared sensor enabled quantitative detection with linear detection ranges of 0.1 to 80 mM, 3 nM to 2 μM, and 1 to 60 mM for Cu(II), Cr(VI), and Ni(II), respectively. In addition, the developed colorimetric sensor achieved lower limits of quantification of 0.1 mM, 3 nM, and 1 mM for Cu(II), Cr(VI), and Ni(II) ions, respectively. The sensor's performance was validated by its excellent selectivity against potential interfering ions and its successful application in the analysis of a real fish sample.

Received 20th December 2025
Accepted 23rd February 2026

DOI: 10.1039/d5ra09860b

rsc.li/rsc-advances

1. Introduction

Although heavy metals are natural resources, the rapid expansion of urbanization and industrialization has resulted in their significantly increased levels, leading to heavy metal contamination. Vehicular traffic, agricultural practices, industrial emissions, aging infrastructure, and improper waste disposal are the main sources of heavy metal contamination. Particularly, the leaching of heavy metals into soil and water and their subsequent introduction into the food chain can damage vital human vital organs and systems due to their bioaccumulation and non-biodegradability.[1,2] Heavy metals are reported as highly potential factors for causing neurological disorders in adults,[3] damage to the kidneys,[4] various cancers,[5] cardiovascular diseases,[6] and respiratory issues.[7] Due to the severe health problems caused by heavy metals, there is an urgent and huge need for developing quick, sensitive, and affordable detection methods for heavy metals. Currently, various conventional methods, such as atomic absorption spectrometry (AAS), high-pressure liquid chromatography (HPLC), and inductively coupled plasma optical emission spectroscopy (ICP-OES), are widely used for the analysis of heavy metals. However, high-cost, long analysis and preparation times, and the requirement of skilled individuals often restrict their wide application.[8]

Recently, biosensors have emerged as efficient and self-integrated analytical devices for providing quantitative or semi-quantitative information. The detection principle in these sensing devices is based on the specific interactions between bioreceptors/receptors with the target.[9,10] Subsequently, different transducers, which employ optical, electrochemical, or piezoelectric-based techniques, are used to convert these interactions into measurable physical and chemical signals. Among these, colorimetric methods represent an affordable and simple analytical method for the analysis of heavy metals.[11,12] Interestingly, a wide range of colorimetric approaches have been implemented on different test strips, such as paper, polymer, silicon, glass, cotton, and even conductive-based substrates.[13] While these miniaturized sensing devices possess numerous advantages, they face some difficulties. For instance, in paper-based colorimetric sensors, the porous and heterogeneous nature of paper often causes uneven fluid flow, uncontrolled spreading of reagents, and variability in color distribution.[14–17] Furthermore, environmental conditions such as humidity, light, and temperature can adversely affect reagent stability and color intensity.[18–21] Similarly, other colorimetric-based sensing system are some limitation such as complex microfabrication.[22–28]

[a]*Asian Nano-Ink Co., Tabriz University of Medical Sciences, Tabriz, Iran*
[b]*Pharmaceutical Analysis Research Center, Tabriz University of Medical Sciences, Tabriz, Iran. E-mail: hasanzadehm@tbzmed.ac.ir*
[c]*Nutrition Research Center, Tabriz University of Medical Sciences, Tabriz, Iran*
[d]*Department of Nanotechnology, Faculty of Chemistry, Urmia University, Urmia, Iran*

Parafilm sheets, a well-characterized class of thermoplastics primarily made up of polyolefins, have received considerable attention in developing colorimetric-based sensing systems due to their accessibility and eco-friendly nature.[29] Currently, parafilm-based colorimetric micro-arrays (PMCAs) demonstrate high potential for advancing healthcare and disease screening, particularly in resource-limited settings. Importantly, the specific advantages of these sensors enable the high-performance quantification of metal ions in food samples without the need for complex preparation procedures.[30] In other words, unlike common fabrication techniques, like photolithographic methods, which need complex steps and expensive instruments,[31,32] using the simple wax printing technology with a wax printer and printing plates offers an eco-friendly and economical approach. The implementation of wax printing on parafilm-based substrates has revolutionized the field of sensing due to its advantages such as simplicity, affordability, and rapidness.[33–35]

In this study, we designed a simple and flexible parafilm-based sensor for monitoring Cu(II), Cr(VI), and Ni(II). In detail, the mechanical strength of the proposed parafilm-based sensor provided a stable sensing substrate, and the use of wax printing technology presented different sensing zones for multiplex detection. For the preparation of PMCA, the parafilm was placed between an iron mold and a magnet to design hydrophilic channels by permeating paraffin.[31] Our validation through the colorimetric analysis of these metal ions in fish samples demonstrated excellent detection limits. Furthermore, the color intensity of sensing zones on the surface of parafilm was analyzed by the eye-dropper color picker software.

2. Experimental section

2.1. Chemicals and instruments

Parafilm sheets were purchased from Bemis Company, USA. Neocuproine,1,5-diphenylcarbazide (DPC) and hydroxylamine (HA) were bought from Sigma-Aldrich, Oakville, Canada. Potassium dichromate ($K_2Cr_2O_7$), acetone, chloroform, H_2SO_4, sodium fluoride (NaF), sodium thiosulfate ($Na_2S_2O_3$), ethanol, dimethyl glyoxime (DMG), Ni(II) chloride ($NiCl_2$), and Cu(II) sulfate ($CuSO_4$) were purchased from Merck, Darmstadt, Germany. The ionic solutions of K(I), Na(I), Ca(II), Mg(II), Cr(VI), Mn(II), Fe(III), Co(II), and Zn(II) were acquired from Chem lab Company, Zedelgem, Belgium. Fresh trout fish was obtained from a local market in Tabriz, Iran. Deionized water was provided by the Shahid Ghazi Pharmaceutical Co., Tabriz, Iran.

The digital images were captured inside a polymeric cylinder (inner diameter: 8.0 cm; height: 10 cm) using a Samsung A2 mobile phone, featuring a powerful 5 MP rear camera equipped with advanced dual autofocus pixels and operating on Android 8.0. The cylinder ensures optimal brightness and mitigates interference from external light sources. In addition, we utilized color picker software (https://play.google.com/store/apps/details?id=gmikhail.colorpicker) and eye-dropper software for the analysis of color intensity on the sensing zones. LOD and LOQ were calculated based on 3Sd per slope or S/N ≈ 3 and 10Sd per slope or S/N ≈ 10, respectively.[36]

2.2. Preparation of fish meat samples

A fish meat extract was prepared by manually squeezing the meat. The produced juice was collected in a clean microtube and maintained in a refrigerator at 4 °C for 24 hours. Subsequently, we centrifuged the juice at 8000 rpm for 10 minutes, separating the supernatant for further analysis. The supernatant was diluted with distilled water in a precise 1 : 2 v/v ratio for analysis.

2.3. Principle of colorimetric sensors based on the PCMA

The performance and efficiency of the PCMA for the colorimetric analysis of Cu(II), Cr(VI), and Ni(II) were validated using fish samples. A metal mold, fabricated by laser machining, was utilized to fabrication of PCMA. The fabricated sensing areas on the parafilm substrate were modified with different reagents through the drop casting technique. The reactions between the reagents and targets on the detection areas were analyzed using the color picker software (see Fig. S1 and VS1). The detection principle of each metal ion is completely discussed in the following sections.

2.3.1. Principle of Cu(II) detection. The determination of Cu(II) relies on the reduction of Cu(II) to Cu(I) by HA and the subsequent formation of a Cu(I)-neocuproine complex, which exhibits an orange color. Particularly, the probe was prepared by mixing 10 μL of HA (0.1 g mL^{-1}) in an acetic acid buffer (6.3 M, pH 4.3) with 10 μL of neocuproine (0.05 g mL^{-1}) in chloroform. Following this, 10 μL of Cu(II) was introduced into the detection zone. The reduction reaction occurs under mildly acidic conditions due to the high efficiency of HA under these conditions. Although, in these buffers, Cu(II) ions may exist as hydrated ions or weak acetate (CH_3COO^-) complexes, but are readily accessible for reduction.[37,38] When the Cu(II) was added to the substrate, an orange color is visible based on the redox reaction of Cu(II) with HA, Neocuproine (Fig. 1A and VS2).

2.3.2. Principle of Cr(VI) detection. In order to prepare a Cr(VI) sensing assay, 10 μL of DPC solution (0.001 g mL^{-1} in 50% v/v acetone) and 10 μL of Cr(VI) solution were added to the detection zone. Afterward, we introduced 1% H_2SO_4 to provide the acidic environment for the colorimetric reaction. Under acidic conditions, Cr(VI) and DPC were reduced and oxidized to Cr(III) and diphenylcarbazide (DPCO), respectively.[39] As shown in Fig. 1B and VS3, the production of Cr(III) results in a color change from pink to purple, which varies with the concentration of Cr(VI).

2.3.3. Principle of Ni(II) detection. The Ni(II) assay was based on the formation of the red Ni-DMG complex. Accordingly, 10 μL of a DMG solution (80 mM in ethanol) was applied to the detection zone through the drop casting technique, followed by the introduction of 10 μL of an aqueous solution containing 0.02 g mL^{-1} of NaF and 0.08 g mL^{-1} of $Na_2S_2O_3$. In the presence of ethanol, the red Ni-DMG complex was produced due to its reaction with Ni(II), as demonstrated in Fig. 1C and VS4. Although fluoride ions (F^-) from NaF could weakly interact with Ni(II), the dominant ligand under the assay conditions was DMG. In addition, the use of sodium thiosulfate ($Na_2S_2O_3$) prevented the formation of interfering Ni hydroxide species.[40]

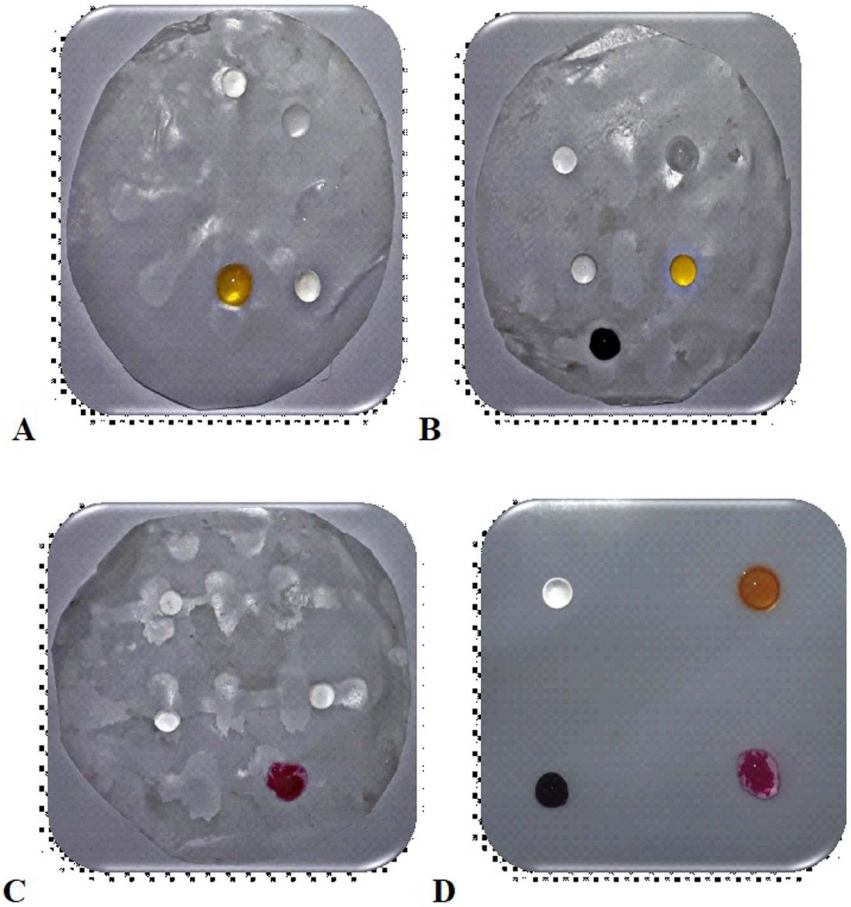

Fig. 1 (A) Colorimetric detection by PMCA for (1) negative control (H_2O), (2) HA/acetic acid buffer (6.3 M), (3) neocuproine/chloroform, (4) Cu(II), (30 mM), (5) HA/neocuproine/Cu(II), (30 mM) in 0 min with volume ration of (1 : 1) v/v. (B) Colorimetric detection by PMCA for (1) negative control (H_2O), (2) diphenyl carbazide/acetone, (3) H_2SO_4 (4) Cr(VI) (5) diphenylcarbazide/H_2SO_4/Cr(VI) in 0 min with volume ratio of (1 : 1) v/v. (C) Colorimetrion detection by PMCA for (1) negative control (H_2O), (2) DMG/ethanol, (3) NaF/$Na_2S_2O_3$ (4) Ni(II) (5) DMG/NaF/$Na_2S_2O_3$/Ni(II) in 0 min with volume ratio of (1 : 1) v/v. (D) Colorimetric detection by PMCA for (1) negative control (H_2O), (2) HA/neocuproine/Cu(II), (3) diphenylcarbazide/H_2SO_4/Cr(VI), (4) DMG/ethanol/NaF/$Na_2S_2O_3$)/Ni(II) in 0 min with volume ratio of (1 : 1) v/v.

To further investigate the color changes induced by these metal ions, the results were repeated at another location on the parafilm sheet (Fig. 1D and VS5).

3. Results and discussion

3.1. Analytical performance

The PCMA was successfully applied for the determination of the three metal ions across a range of concentrations. The colorimetric assay of Cu(II) relied on redox reactions and complex formation, where Cu(II) is reduced to Cu(I) in the presence of HA (see results in VS5). This mechanism was visually observable through color changes from light orange to dark orange with increasing concentrations of Cu(II). Fig. 2A and B show the calibration curves of Cu(II) obtained in the concentration range from 5 μM to 80 mM. In addition, the linear regression equation found for the colorimetric detection of Cu(II) based on the PCMA was

$$y = -0.0011(C_{Cu(II)}) + 0.1484,\ R^2 = 0.9667.$$

The accuracy of the colorimetric detection of Cr(VI) was observed based on the revelation of purple color. The intensity of color increased from light to dark purple in response to increasing the Cr(VI) concentration from 3 nM to 0.002 mM (Fig. 2C, D and VS6). For the reported PCMA-based colorimetric sensor, LLOQ was determined to be 3 nM with an average relative standard deviation (RSD) of 0.9127. The colorimetric detection of Ni(II) based on the PCMA was validated by the distinct pinkish color formation (VS7). As depicted in Fig. 2E and F, the color changed from light pink to dark pink in response to Ni(II) concentrations ranging from 2 μM to 60 mM. The LLOQ and R^2 values were calculated to be 2 μM and 0.9715, respectively.

In addition to analysis by the naked eyes, an analysis based on the eye-dropper software was done and is completely summarized in Table S1. Each group included nine colorimetric indicators characterized by their red-green-blue (RGB) values and hex codes, color names, peak wavelengths (λ), and LLOQ. The RGB results obtained by the smartphone were validated by the eye-dropper software (https://instant-eyedropper.com/) (Table S1, SI).

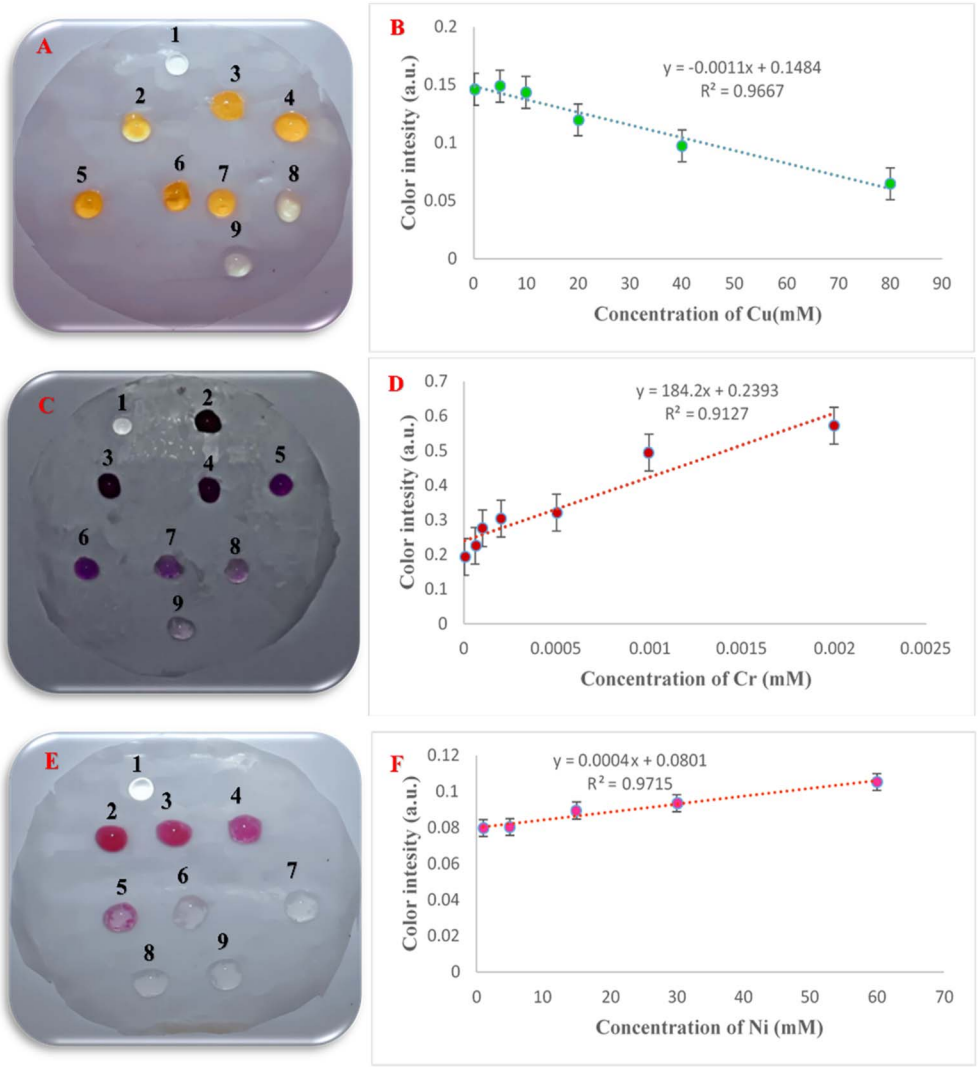

Fig. 2 (A) Photographs of the Cu(II) colorimetric response in the concentration range 0.1 mM to 80 mM (B) calibration curves of Cu(II). (C) Colorimetric response of Cr(VI) in the concentration range 3 nM to 0.002 mM (D) calibration curves of Cr(VI). (E) Colorimetric response of Ni(II) in the concentration range 1 mM to 60 mM. (F) Calibration curves of Ni(II).

3.2. Real sample analysis

The feasibility of the developed PCMA-based sensing approach for practical applications was analyzed using fish meat. In order to prepare real samples, the prepared supernatant from fish meat extract was spiked with various concentrations of candidate metal ions (1 : 1). In addition, different incubation times, including 0, 60, 120, and 180 min at room temperature, were used to demonstrate the stability of real matrices. As presented in Fig. S1 and VS8–S10, in the presence of different targets on the surface of modified sensing zones, the color of sensing areas changed, and this was captured by a smartphone and analyzed by the color picker software.

For Cu(II) detection, the developed PCMA demonstrated a linear detection range of 5 μM to 80 mM and an LLOQ of 5 μM (Fig. S2E and VS11). In addition, a regression equation ($y = 0.0799(C_{Cu(II)}) + 0.002$) and an R^2 value of 0.9154 were obtained based on a calibration curve. Under optimum conditions, the calibration curve for Cr(VI) detection was attained by plotting the color intensity *versus* the concentration of Cr(VI), resulting in a regression equation of $y = 0.1987\ (C_{Cr(VI)}) + 3.3068$ and an R^2 value of 0.9566. As shown in Fig. S3 and VS12, the PCMA demonstrated a linear detection range of 0.2 μM to 0.1 mM and an LLOQ of 0.2 μM toward Cr(VI) sensing. Also, linear range of 2 μM to 60 mM and of 2 μM was obtained for the detection of Ni(II) (Fig. S4 and VS13).

A comparison of the captured images after different incubation times demonstrated that the color changes are consistent even at 180 min. This ability makes the PCMA a highly promising sensor for practical applications.

A comparison of the analytical performances of sensors developed for the detection of metal ions is summarized in Table 1. The results of our parafilm-based sensor demonstrated significant advancements when compared with the existing paper-based sensors for candidate metal ion analyses highlighted in the literature. As indicated in Table 1, most paper-based sensors are primarily focused on detecting Cr(VI), Cu(II),

Table 1 Comparison of the analytical performances of previously developed sensors with those of our sensor in the detection of candidate metal ions[a]

Target	Probe	Color capturing instrument	Sample	LOD/LOQ/LLOD/LLOQ	Ref.
Ni(II), Cr(VI), and Hg(II)	Silane compounds terminating with NH_2, COOH, and SH	Smartphone camera	Water	0.24 ppm, 0.18 ppm, and 0.19 ppm	41
Lead(II), mercury(II), cadmium(II), and arsenic(III)	Aptamers	Smartphone camera	Apple and lettuce	4.20 nM, 1.70 nM, 2.04 nM, and 1.65 nM	42
Fe(III), Ni(II), Cr(VI), Cu(II), Al(III), and Zn(II)	NR	Smartphone camera	Mixtures and environmental samples	0.2, 0.3, 0.1, 0.03, 0.08, and 0.04 mg L^{-1}	43
Ni(II), Cu(II), and Fe(III)	NR	Smartphone camera	Water	2 and 6.67 ppm, 0.3 and 1 ppm	44
Fe, Ni, Cu, Zn, Cd and Pb	Screen-printed electrochemical paper-based device	Hewlett-Packard Scanjet G4050 office scanner	River water	0.1, 0.3, and 0.2 mg L^{-1}	45
Hg(II)	AgNPs	Naked eyes	Water	0.1 mg L^{-1}	46
Cu(II) and Zn(II)	NBD-Cl and Girard's reagent	Smartphone camera	Rainwater	Down to 0.77 μM and 1.66 μM	47
Cu(II), Co(II), Ni(II), Hg(II), and Mn(II)	Bc, DMG, DTZ, and PAR as complexing agents	Scanner (Brother MFC-8370DN)	Drinking, tap, and pond water	0.32, 0.59, 5.87, 0.20, and 0.11 mg L^{-1}	48
Zn(II) and Co(II)	Paper substrate using polyvinyl chloride	CanoScan LiDE 220 color scanner	Water	0.03 and 0.08 mg L^{-1}	49
Cr(VI), Cu(II), and Ni(II)	Different reagents	Naked eyes and smartphone camera	Fish	0.1 mM, 3 nM, and 0.1 mM	This work

[a] Abbreviations: Bc, bathocuproine; DMG, dimethylglyoxime; DTZ, dithizone; PAR, 4-(2-pyridylazo) resorcinol; AgNPs, silver nanoparticles; NH2, amine; COOH, carboxyl; SH, thiol; and NBD-Cl, 4-chloro-7-nitro-2,1,3-benzoxadiazole.

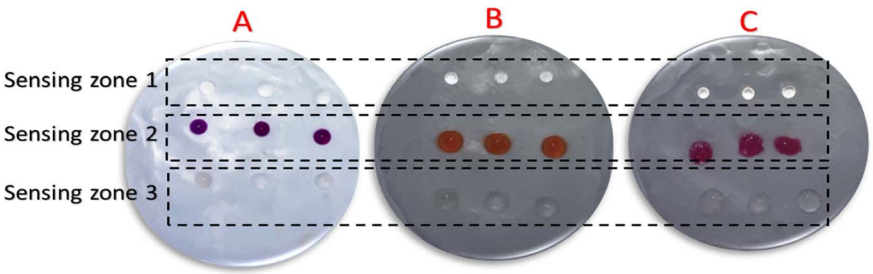

Fig. 3 Images of the selectivity of the PCMA-based sensor towards (A) Cr(VI), (B) Cu(II), and (C) Ni(II) and comparison with (1) negative controls, (2) targets, and (3) complex cocktail solutions.

Hg(II) and Ni(II) ions in water samples. In order to use these sensors in food analysis, several complex processes, such as homogenization, filtration, and pH adjustments, need to performed. The proposed platform reduces the need for substantial quantities of solvents and analytes. This ability highlights its potential as a groundbreaking solution in offering a highly efficient sensing approach for metal ion detection in food safety.

3.3. Selectivity assays of Cr(VI), Cu(II), and Ni(II) using the PCMA

The selectivity of the developed assay was evaluated based on three innovative detection zones in the presence of various potential interfering ions that could affect the accuracy and precision of the sensor. In detail, zone 1 served as the negative control, and zone 2 was able to identify Cr(VI) at a low concentration (0.0001 mM), alongside Cu(II) at 20 mM and Ni(II) at 15 mM (Fig. 3). Furthermore, zone 3 analyzed a complex cocktail of solutions, containing mix 1 [(Ca(II), Fe(III), Li(I), and Zn(II)], mix 2 [(Mn(II), Mg(II), Na(I), and K(I)], and mix 3 which is a combination of all ions from mix 1 and mix 2. Note that all ions in the cocktail solutions were at a concentration of 20 mM.

The solutions were drop-casted onto each modified zone, and the color intensity was analyzed following the reaction. As illustrated in Fig. 3A–C, each detection zone exhibited distinct color changes in the presence of its corresponding target analytes (VS14–S16). Remarkably, the reported sensor maintained its selectivity without interference from cocktail solutions containing multiple metal ions.

4. Conclusion

In summary, a simple, affordable, flexible, and multiple-ion detection sensor based on parafilm was established for

detecting Cu(II), Cr(VI), and Ni(II) ions. The developed optical probe demonstrated color changes towards metal ions on the surface of the sensing zone. The color change on the surface of the designed sensor could be identified by the naked eye and captured by a specific smartphone software. The developed PCMA demonstrated excellent sensitivity and wide linear detection ranges of 0.1 mM to 80 mM for Cu(II), 3 nM to 0.002 mM for Cr(VI), and 1 mM to 60 mM for Ni(II). In addition, the designed sensor demonstrated excellent reliability due to its selectivity in the presence of interfering ions and acceptable analytical performance in a real fish meat sample. One challenge (limitation) in using this colorimetric sensor is that the reaction responsible for the color change occurs slowly, and this color change disappears after a limited time (maximum 60 minutes) at room temperature. This is because of the potential solvent evaporation, which limits its use in the analysis process. Despite the promising properties of the PCMA, future efforts for its standardized manufacturing, biocompatibility enhancements, and integration with readout technologies are necessary. Addressing these challenges will be essential for the transformation of the PCMA from the laboratory to practical applications.

Conflicts of interest

There are no conflicts to declare.

Data availability

Access to the data used in this study is available upon request and may be subject to approval by the data provider. Restrictions may apply to the availability of these data, which were used under license for this study. Interested parties are encouraged to contact the corresponding author for further information on accessing the data. All data are available within the manuscript and supplementary information (SI). Supplementary information: Fig. S1: photographs of modified PCMA with (1) fish meat, (2) H_2O, (3) HA/neocuproine/Cu(II), (4) diphenyl carbazide/H_2SO_4/Cr(VI), (5) dimethylglyoxime/ethanol/NaF/$Na_2S_2O_3$/Ni(II). Fig. S2 (A–D): photographs of the modified PCMA at four incubation times, including 0, 60, 120, and 180 minutes, with (1) H_2O, (2) fish meat, and (3–10) fish meat/HA/acetic acid buffer/neocuproine/chloroform/Cu(II) at concentrations of 0.005, 0.01, 0.1, 5, 10, 20, 40, and 80 mM. (E) calibration curves ($n = 3$, SD = 2.046 ± 0.2). Fig. S3 (A–D): photographs of the modified PCMA at four incubation times, including 0, 60, 120, and 180 minutes, with (1) H_2O, (2) fish meat, and (3–10) fish meat/diphenyl carbazide/acetone/H_2SO_4/Cr(VI) at concentrations of 0.0002, 0.0005, 0.001, 0.002, and 0.1 mM. (E) calibration curves ($n = 3$, SD = 2.063 ± 0.2). Fig. S4 (A–D): photographs of the modified PCMA at four incubation times, including 0, 60, 120, and 180 minutes, with (1) H_2O, (2) fish meat, and (3–10) fish meat/dimethylglyoxime/ethanol/NaF/$Na_2S_2O_3$/Ni(II) at concentrations of 0.002, 0.01, 0.1, 1, 5, 15, and 30 mM. (E) calibration curves. ($n = 3$, SD = 1.79 ± 0.2). Table S1: analytical summary of colorimetric data and detection sensitivity our study for detecting candidate metal ions. See DOI: https://doi.org/10.1039/d5ra09860b.

Acknowledgements

We are grateful for the financial assistance for this work from the Research Center for Pharmaceutical Nanotechnology, Tabriz University of Medical Sciences (77567).

References

1 F. N. Chowdhury and M. M. Rahman, Source and distribution of heavy metal and their effects on human health, *Heavy Metal Toxicity: Human Health Impact and Mitigation Strategies*, Springer, 2024, pp. 45–98.
2 H. K. Kordasht, M. Pazhuhi, M. Hasanzadeh, N. Shadjou, N. H. Voelcker and A. Nilghaz, Ensuring food and water safety using magnetic mesoporous silica nanomaterials-based biosensors, *TrAC, Trends Anal. Chem.*, 2024, **181**, 117998.
3 Q. Rehman, K. Rehman and M. S. H. Akash, Heavy metals and neurological disorders: from exposure to preventive interventions, *Environmental Contaminants and Neurological Disorders*, Springer, 2021, pp. 69–87.
4 K. Brindhadevi, D. Barceló, N. T. L. Chi and E. R. Rene, E-waste management, treatment options and the impact of heavy metal extraction from e-waste on human health: Scenario in Vietnam and other countries, *Environ. Res.*, 2023, **217**, 114926.
5 M. Radfard, H. Hashemi, M. A. Baghapour, M. R. Samaei, M. Yunesian, H. Soleimani and A. Azhdarpoor, Prediction of human health risk and disability-adjusted life years induced by heavy metals exposure through drinking water in Fars Province, Iran, *Sci. Rep.*, 2023, **13**, 19080.
6 S. Nucera, M. Serra, R. Caminiti, S. Ruga, L. C. Passacatini, R. Macrì, F. Scarano, J. Maiuolo, R. Bulotta and R. Mollace, Non-essential heavy metal effects in cardiovascular diseases: an overview of systematic reviews, *Front. Cardiovasc. Med.*, 2024, **11**, 1332339.
7 R. Bharti and R. Sharma, Effect of heavy metals: An overview, *Mater. Today: Proc.*, 2022, **51**, 880–885.
8 K. Jomova, S. Y. Alomar, E. Nepovimova, K. Kuca and M. Valko, Heavy metals: toxicity and human health effects, *Arch. Toxicol.*, 2025, **99**, 153–209.
9 H. Kholafazad-Kordasht, M. Hasanzadeh and F. Seidi, Smartphone based immunosensors as next generation of healthcare tools: Technical and analytical overview towards improvement of personalized medicine, *TrAC, Trends Anal. Chem.*, 2021, **145**, 116455.
10 H. K. Kordasht, M. Hasanzadeh, F. Seidi and P. M. Alizadeh, Poly (amino acids) towards sensing: Recent progress and challenges, *TrAC, Trends Anal. Chem.*, 2021, **140**, 116279.
11 S. Hosseinikebria, M. Khazaei, M. Dervisevic, M. A. Judicpa, J. Tian, J. M. Razal, N. H. Voelcker and A. Nilghaz, Electrochemical biosensors: The beacon for food safety and quality, *Food Chem.*, 2025, **475**, 143284.

12 M. A. Mangi, H. Elahi, A. Ali, H. Jabbar, A. B. Aqeel, A. Farrukh, S. Bibi, W. A. Altabey, S. A. Kouritem and M. Noori, Applications of piezoelectric-based sensors, actuators, and energy harvesters, *Sens. Actuator Rep.*, 2025, **9**, 100302.
13 H. Lu, M. Li, A. Nilghaz, L. Li, G. Chen, Y. Jiang and J. Tian, Paper-based analytical device for high-throughput monitoring tetracycline residue in milk, *Food Chem.*, 2021, **354**, 129548.
14 M. M. Gong and D. Sinton, Turning the page: advancing paper-based microfluidics for broad diagnostic application, *Chem. Rev.*, 2017, **117**, 8447–8480.
15 L. Yan-Qi and F. Liang, Progress in paper-based colorimetric sensor array, *Chin. J. Anal. Chem.*, 2020, **48**, 1448–1457.
16 Y. Hou, C.-C. Lv, Y.-L. Guo, X.-H. Ma, W. Liu, Y. Jin, B.-X. Li, M. Yang and S.-Y. Yao, Recent advances and applications in paper-based devices for point-of-care testing, *J. Anal. Test.*, 2022, **6**, 247–273.
17 A. Ko and C. Liao, based colorimetric sensors for point-of-care testing, *Anal. Methods*, 2023, **15**, 4377–4404.
18 S. Kumar, J. B. Kaushal and H. P. Lee, Sustainable sensing with paper microfluidics: Applications in health, environment, and food safety, *Biosensors*, 2024, **14**, 300.
19 E. W. Nery and L. T. Kubota, Sensing approaches on paper-based devices: a review, *Anal. Bioanal. Chem.*, 2013, **405**, 7573–7595.
20 S. Patel, R. Jamunkar, D. Sinha, T. K. Patle, T. Kant, K. Dewangan and K. Shrivas, Recent development in nanomaterials fabricated paper-based colorimetric and fluorescent sensors: A review, *Trends Environ. Anal. Chem.*, 2021, **31**, e00136.
21 F.-Q. Yang and L. Ge, *Colorimetric Sensors: Methods and Applications*, MDPI, 2023, pp. 9887.
22 L. Agiotis, I. Theodorakos, S. Samothrakitis, S. Papazoglou, I. Zergioti and Y. Raptis, Magnetic manipulation of superparamagnetic nanoparticles in a microfluidic system for drug delivery applications, *J. Magn. Magn. Mater.*, 2016, **401**, 956–964.
23 I. Giouroudi and F. Keplinger, Microfluidic biosensing systems using magnetic nanoparticles, *Int. J. Mol. Sci.*, 2013, **14**, 18535–18556.
24 M. A. Gijs, F. Lacharme and U. Lehmann, Microfluidic applications of magnetic particles for biological analysis and catalysis, *Chem. Rev.*, 2010, **110**, 1518–1563.
25 F. Ender, D. Weiser, A. Vitéz, G. Sallai, M. Németh and L. Poppe, In-situ measurement of magnetic nanoparticle quantity in a microfluidic device, *Microsyst. Technol.*, 2017, **23**, 3979–3990.
26 M. A. Maleki, M. Soltani, N. Kashaninejad and N.-T. Nguyen, Effects of magnetic nanoparticles on mixing in droplet-based microfluidics, *Phys. Fluids*, 2019, **31**, 032001.
27 Y. Yu, C. Zhang, X. Yang, L. Sun and F. Bian, Microfluidic Synthesis of Magnetic Nanoparticles for Biomedical Applications, *Small Methods*, 2025, **9**, 2401220.
28 N. Van Tuan, H. A. Tam, N. T. Ngoc, V. N. Thuc, N. K. Binh, N. T. P. Thao, D. T. Hien, B. T. Sang, N. H. Nam and V. D. Lam, High-efficiency microfluidic chip integrated with micro-patterned planar spiral sensors for magnetic nanoparticle detection, *Lab Chip*, 2025, **25**, 2977–2989.
29 Z. Li, Y.-H. Cheng, C. Chande, S. Chatterjee and S. Basuray, A highly sensitive, easy-and-rapidly-fabricable microfluidic electrochemical cell with an enhanced three-dimensional electric field, *Anal. Chim. Acta*, 2022, **1232**, 340488.
30 F. Bahavarnia, M. B. Behyar, A. Nilghaz, M. Hasanzadeh and N. Shadjou, Colorimetric chemosensing of Riboflavin using polymeric micro-array reinforced by silver nanoparticle: State-of-the-art on one-drop biomedical analysis, *Sci. Rep.*, 2025, **15**, 25138.
31 Z. Li, N. Haridas, S. Kaaliveetil, Y.-H. Cheng, C. Chande, V. Perez, A. K. Miri and S. Basuray, Low-cost rapid prototyping for microfluidics using Parafilm®-based microchannels for low resource settings, *Sens. Actuators, B*, 2024, **404**, 135212.
32 L. Meng, D. Cao, J. O. Pedersen, G. Greczynski, V. Rogoz, W. Limbut and M. Eriksson, Seamless Integration of Laser-Induced Papertronics with Parafilm-Based Microfluidics as a Versatile Paper-Based Electroanalytical Platform, ACS Applied Materials & Interfaces, *ACS Appl. Mater. Interfaces*, 2025, **17**, 39719–39731.
33 C.-H. Lin, J.-H. Lin, C.-F. Chen, Y. Ito and S.-C. Luo, Conducting polymer-based sensors for food and drug analysis, *J. Food Drug Anal.*, 2021, **29**, 544.
34 H. Lim, A. T. Jafry and J. Lee, Fabrication, flow control, and applications of microfluidic paper-based analytical devices, *Molecules*, 2019, **24**, 2869.
35 P. He, *Development of Paper-Based Point-Of-Care Biosensors by Laser-Based Direct-Write Processes*, University of Southampton, 2017.
36 https://www.fda.gov/downloads/Drugs/Guidances/ucm070107.pdf.
37 M. Zheng, J. Zhang, P. Wang, H. Jin, Y. Zheng and S. Z. Qiao, Recent advances in electrocatalytic hydrogenation reactions on copper-based catalysts, *Adv. Mater.*, 2024, **36**, 2307913.
38 H. Lee, H.-J. Lee, J. Seo, H.-E. Kim, Y. K. Shin, J.-H. Kim and C. Lee, Activation of oxygen and hydrogen peroxide by copper (II) coupled with hydroxylamine for oxidation of organic contaminants, *Environ. Sci. Technol.*, 2016, **50**, 8231–8238.
39 H. Kholafazad, M. Pazhuhi, M. Hasanzadeh, N. H. Voelcker, N. Shadju and A. Nilghaz, Cellulosic-Based Microneedles for Sensing Heavy Metals in Fish Samples, *Carbohydr. Polym. Technol. Appl.*, 2025, 100853.
40 A. Ferancová, M. K. Hattuniemi, A. M. Sesay, J. P. Räty and V. T. Virtanen, Complexation of Ni(II) by dimethylglyoxime for rapid removal and monitoring of Ni(II) in water, *Mine Water Environ.*, 2017, **36**, 273–282.
41 J. P. Devadhasan and J. Kim, A chemically functionalized paper-based microfluidic platform for multiplex heavy metal detection, *Sens. Actuators, B*, 2018, **273**, 18–24.
42 M. Yuan, C. Li, Y. Zheng, H. Cao, T. Ye, X. Wu, L. Hao, F. Yin, J. Yu and F. Xu, A portable multi-channel fluorescent paper-based microfluidic chip based on smartphone imaging for simultaneous detection of four heavy metals, *Talanta*, 2024, **266**, 125112.

43 F. Li, Y. Hu, Z. Li, J. Liu, L. Guo and J. He, Three-dimensional microfluidic paper-based device for multiplexed colorimetric detection of six metal ions combined with use of a smartphone, *Anal. Bioanal. Chem.*, 2019, **411**, 6497–6508.

44 P. Aryal, E. Brack, T. Alexander and C. S. Henry, Capillary flow-driven microfluidics combined with a paper device for fast user-friendly detection of heavy metals in water, *Anal. Chem.*, 2023, **95**, 5820–5827.

45 H. A. Silva-Neto, T. M. Cardoso, C. J. McMahon, L. F. Sgobbi, C. S. Henry and W. K. Coltro, Plug-and-play assembly of paper-based colorimetric and electrochemical devices for multiplexed detection of metals, *Analyst*, 2021, **146**, 3463–3473.

46 M. L. Budlayan, J. Dalagan, J. P. Lagare-Oracion, J. Patricio, S. Arco, F. Latayada, T. Vales, B. Baje, A. Alguno and R. Capangpangan, Detecting mercury ions in water using a low-cost colorimetric sensor derived from immobilized silver nanoparticles on a paper substrate, *Environ. Nanotechnol., Monit. Manage.*, 2022, **18**, 100736.

47 M. El-Maghrabey, S. Seino, N. Kishikawa and N. Kuroda, The Development of a Selective Colorimetric Sensor for Cu2+ and Zn2+ in Mineral Supplement with Application of a Smartphone Paper-Based Assay of Cu^{2+} in Water Samples, *Sensors*, 2024, **24**, 7844.

48 P. Kamnoet, W. Aeungmaitrepirom, R. F. Menger and C. S. Henry, Highly selective simultaneous determination of Cu(II), Co(II), Ni(II), Hg(II), and Mn(II) in water samples using microfluidic paper-based analytical devices, *Analyst*, 2021, **146**, 2229–2239.

49 H. Sharifi, J. Tashkhourian and B. Hemmateenejad, Identification and determination of multiple heavy metal ions using a miniaturized paper-based optical device, *Sens. Actuators, B*, 2022, **359**, 131551.